NESCOFI@BTF

NEutron Spectrometry in COmplex FIelds @ Beam Test Facility

2013 Activity Report

R. Bedogni (70%), D. Bortot (50%), B. Buonomo (20%), A. Esposito (30%), G. Mazzitelli (20%), L. Quintieri (20%), A. Gentile (40%), M. Chiti (20%).
INFN - LNF

J.M. Gomez-Ros (40%)
CIEMAT, Madrid / associato LNF

M.V. Introini, A. Pola
INFN-Milano / Politecnico di Milano

Index

1. *Introduction and motivation*

NESCOFI@BTF started in 2011 with the aim of developing innovative neutron sensitive instruments for the spectrometric and dosimetric characterization of neutron fields, intentionally produced or present as parasitic effects, in particle accelerators used in industry, research and medical fields. Neutron spectra in these fields range from thermal (1E-8 MeV) to tens or hundreds MeV, thus spanning over more than 10 decades in energy. As shown in Fig. 1, only the multi-sphere spectrometer (or Bonner Sphere spectrometer) is able to simultaneously determine all energy components over such a large energy interval. The main disadvantage of this spectrometer is the need to sequentially expose a considerable number (usually more than 10) of detector+moderator configurations, thus leading to time-consuming irradiation sessions. The idea behind NESCOFI is to provide real-time spectrometers able to simultaneously provide all energy components in a single irradiation. These could be employed for:

(1) Monitoring the neutron fields in terms of energy-integrated neutron flux and spectral neutron flux in energy intervals of interest.

(2) Active real-time control of possible deviations from nominal field properties and of possible modifications induced by materials introduced in the radiation field (samples, waste elements, materials to be tested).

The final users of the NESCOFI products will be a variety of facilities interested to monitor not only the intensity of a neutron beam, but also –and simultaneously- its energy and/or direction distribution (chip-irradiation, material science neutron beam-lines, reference neutron fields, research and cancer therapy facilities).

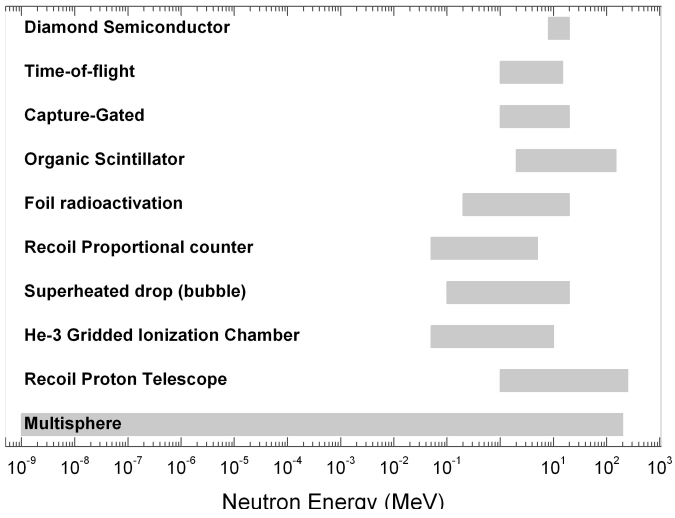

Fig. 1. Energy interval covered by different available neutron spectrometry techniques.

The basic idea behind the project is to exploit the moderation of neutrons in hydrogenated materials, as extensively done in Bonner Sphere spectrometers, but new designs and computational methods have been

introduced. Particularly, instead of estimating the neutron energy distribution by exposing different detector+moderator configurations, this project aims at a single moderator embedding several "direct reading" thermal neutron detectors at different positions. The energy or angle distribution of the neutron field will be obtained using unfolding algorithms relying on the device response matrix and on the reading of the different detectors. This "unfolding" problem has a number of analogies with the spectrum reconstruction with Bonner Sphere spectrometers, for which a special code called FRUIT [1,2] (FRascati Unfolding Interactive Tools) was developed at LNF.

The NESCOFI project planned to be completed in three years (2011-2013), organized as follows:

2011: (1) optimization (via Monte Carlo simulation) of the spectrometer geometry and development of a prototype working with passive detectors
(2) establishment of a reference neutron field for testing purposes, namely the photo-neutron beam from the n@BTF facility at the LNF.

2012: Development of suitable "direct reading" (or active) thermal neutron detectors to be embedded in the final spectrometers

2013: Establishment and calibration of the final spectrometers

2. 2011 and 2012 activities

See 2011 and 2012 annual reports and website http://www.lnf.infn.it/acceleratori/public/nescofi/

3. 2013 activities

3.1 *Introduction to 2013 activities*

The 2013 activities were focused on achieving two milestones, namely:

Sept. 2013 Building SP^2 and CYSP with associated DAQ systems

Dec. 2013 electronics testing; spectrometer calibration (according to possibilities)

In addition, the design, production and response characteristics of the active thermal neutron detectors are now consolidated. Two types of thermal neutron detectors are now standardized, namely the TNPD (Thermal neutron pulse detector) and TNRD (thermal neutron rate detector). These are described in Para 3.3 and 3.4.

Both SP^2 and CYSP spectrometers were built, equipped with TNPD detectors and the electronics were tested on time.

Because of the restriction on funds for travelling (assigned 6.5 k€, compared to more than 20 k€ requested), the complete calibration to monochromatic beams was achieved for the CYSP only, by means of a collaboration agreement with NPL (Teddington, UK) that assigned one week beam time on the mono-

chromatic neutron facility upon payment of a reduced fee (5 k€ compared to 15 k€ regular tariff).
Results are described in Para. 3.5.2.
Concerning SP^2 a partial calibration was achieved using a reference Am-Be source at LNF (spectrum ranging from 0.1 to 12 MeV) and a quasi mono-chromatic 14 MeV beam freely provided by ENEA. Results are described in Para. 3.6.2. and 3.6.3.
In addition to the SP^2 and CYSP development activity, a side activity has started to disseminate the newly developed thermal neutron detectors in the medical sector, particularly for the neutron dosimetry of the patient undergoing radiotherapy treatment. This activity was co-funded by the Sevilla University. See Para. 3.7. Following the satisfactorily results from this test, the system formed by a single TNRD and its DAQ electronics was extended to five parallel detectors working in parallel to simultaneously measure neutron doses in multiple organs (Co-funded by Sevilla University).
The results of 2013 physics activity were submitted to the NEUDOS-12 Conference (Aix en Provence, France) and are under publication in Radiat. Prot. Dosim. Seven papers were submitted, 4 orals and 3 poster. Other two contributions (one invited and one poster), mainly related to the neutron monitoring in medical sector, were presented to the SEFM 19 - SEPR 14 conference (Caceres, Spain).

3.2 *Active Thermal neutron detectors (ATND)*

One of the key activities of NESCOFI@BTF, performed in the second year (2012), was the development of active thermal neutron detectors (ATND) to be embedded in the CYSP and SP^2 moderating geometries to yield the final spectrometers. The following requirements needed to be followed:

- Miniaturization: the target dimension for a single detector is in the order of one cm;
- Sensitivity and linearity: the spectrometers should work with dose rates ranging from μSv/h up to Sv/h;
- Excellent photon rejection;
- Low-cost: a single CYSP includes only seven ATND, but an SP^2 includes thirty-one of them. This constraint excluded in practice any commercially available active TNDs.

The final decision was to develop customized detectors by making low-cost commercial solid-state devices sensitive to thermal neutrons. A customized physical-chemical process was developed to deposit thin layers (tens of microns) of compounds including large fraction of elements (like ^{10}B or ^{6}Li) with high cross section for (neutron, charged particle) capture reactions. The resulting thermal neutron sensitive detectors, after the in-house sensitization process, are shown in Fig. 2. The white layer is the (n, charged particle) converter. The silicon diode detects the resulting charged particles.

Figure 2. The ATNDs, after the in-house sensitization process. The white layer is the (n, charged particle) converter. The silicon diode detects the resulting charged particles.

To cover the broad range of neutron field intensity given above, the NESCOFI group decided to propose TWO different devices, both based on the solid state devices shown in Fig. 2, having different levels of cost and sensitivity.

3.3 *The "thermal neutron pulse detector" TNPD*

The so called "thermal neutron pulse detector" TNPD [3] produces a pulse height distribution, from which the thermal neutron fluence can be derived. Analog signals from TNPDs are sent to the multi-detector board (developed within NESCOFI@BTF) shown in Fig. 3. This includes eight independent spectrometry chains. Each one is composed by a bias regulator, a charge preamplifier and a shaper amplifier. The

amplified signals are transmitted to multi-channel commercial ADC (NI USB 6366). Each analogue signal is digitized with 16 bits and sampling rate 2 Msamples/s.

From the pulse height distribution the neutron-to-photon discrimination is performed and the net thermal neutron signal is extracted. Typical thermal neutron sensitivity: 0.03 cm^2 (counts per unit fluence).

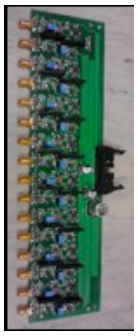

Figure 3. Multi-detector NESCOFI acquisition board. Up to 16 detectors can be controlled through SMA connectors. For every detector a charge preamplifier and a shaper amplifier allow adapting, guassian-shaping an magnifying the charge pulses produced in the semiconductor based thermal neutron detectors. The amplified signals are sent to a multi-channel digitizer (NI USB 6366) controlled through a Labview program. The control software allows simultaneous spectrum calculation for all detectors.

The converted employed in both TNPD and TNRD (conventionally called C2 in 2012 Report) was developed and optimized in thickness with the special aim of reducing the photon sensitivity without compromising the thermal neutron sensitivity.

As shown in Figure 4, the use of converter C2 does not require to expose a double detector because the photon-induced signal falls well below the spectral region of interest for thermal neutrons.

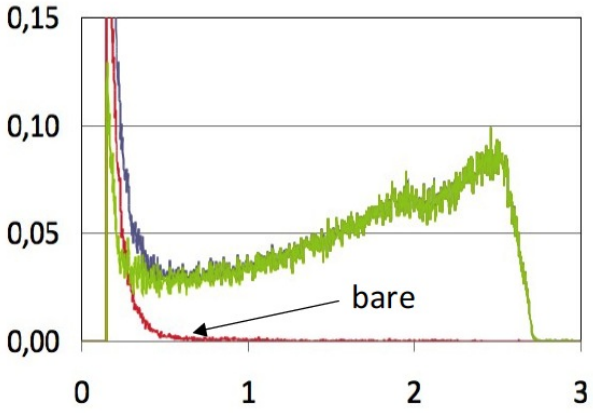

Figure 4. Spectrum of energy deposited in the TNPD. The label “bare” denotes the uncovered detector. The Blue spectrum is the “covered” detector. The green spectrum is the “covered” – “bare” spectrum. X axis is

pulse height (V) and Y axis is number of pulses (a.u.).

Characteristics of TNPD are:

- Different detector thicknesses are easy to fabricate and well controllable;
- Optimal sensitivity obtained: 0.026 counts per unit thermal fluence (cm^2);
- Fabrication reproducibility <10%;
- Radiation damage observed for integrated thermal neutron fluence 3E+12 cm^{-2} (measured at TRIGA reactor, ENEA Casaccia).
- A single exposure is sufficient to discriminate the thermal neutron component from the photon one.

The TNPD was further tested against a well-established detector, the ^{6}LiI(Eu) scintillator, at the centre of a set of Bonner spheres. The test was performed at TSL Uppsala [3] where a wide neutron spectrum is produced by bombarding a Be target with 30 MeV protons. Figure 5 demonstrate that the neutron spectra derived with the ^{6}LiI(Eu) scintillator or the TNRD at centre of the Bonner spheres are equivalent.

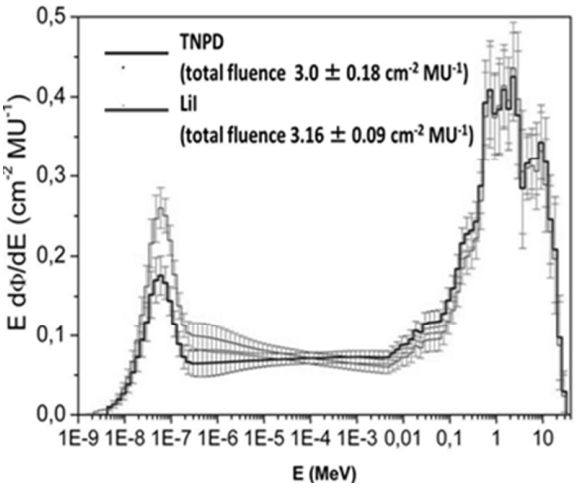

Figure 5. Neutron spectra derived with the ^{6}LiI(Eu) scintillator or the TNRD at centre of the Bonner spheres at the TSL facility (30 MeV protons on Be target). Spectra are in equi-lethargy representation.

3.4 *The "thermal neutron rate detector" TNRD*

The so called "thermal neutron rate detector" TNRD [4] produces a DC voltage level that is proportional to the thermal neutron flux. Adequate photon rejection is achieved through an intrinsic compensation effect. The lowest measurable thermal neutron flux is <100 $cm^{-2}s^{-1}$.

With respect to the TNPD, the TNRD shows simplified readout and reduced cost. By contrast its sensitivity is lower than that of the TNPD.

The TNRD active area is one cm^2 and its overall dimensions are approx. 1.5 cm x 1 cm x 0.4 cm. Its output is a DC voltage, which is proportional to the thermal neutron fluence rate (for this reason the device is called "rate detector"). This signal is amplified in a low-voltage electronics module especially developed by the project team. The amplifier output is sent to a programmable ADC (NI USB-6218 BNC, 16 bit, up to 250 kS/s) controlled by a PC through a LabView application. The detector and its typical time-dependent output are shown in Figs. 6 and 7.

Figure 6. The thermal neutron rate detector (TNRD).

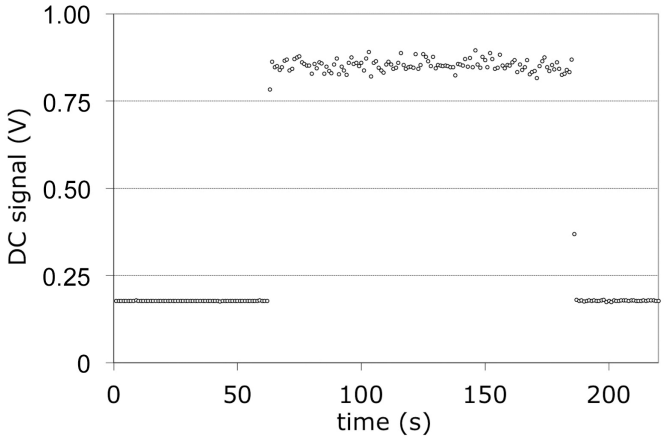

Figure 7. Time-dependent output of the TNRD when exposed in an ex-core thermal neutron beam from the ENEA Casaccia TRIGA reactor at power 46 kW. The step is produced when opening and closing the

neutron shutter. The conventional fluence rate is about 6E+4 $cm^{-2}s^{-1}$. The constant voltage level measured in the "shutter closed" configuration corresponds to an offset in the operational amplifier-based circuit used to treat the detector signal.

Conventional thermal flux ($cm^{-2}s^{-1}$)	1270±40
True thermal flux ($cm^{-2}s^{-1}$)	1440±40
Total neutron flux ($cm^{-2}s^{-1}$)	3300±100
"Non thermal" contribution to detector reading	1.6%
Photon kerma rate ($\mu Gy \cdot h^{-1}$)	44±2

Table 1. Results of the MCNPX simulations for the moderating cylinder. The photon kerma rate, almost completely due to the 2.2 MeV photons from neutron capture reactions in hydrogen, was measured with TLD-700 passive detectors previously calibrated in a reference ^{137}Cs field.

TNRDs are individually calibrated in the moderating assembly depicted in Fig. 8. This consists in a high-density polyethylene cylinder with diameter = height = 25 cm associated with a calibrated ^{241}Am-Be source (2.09E+6 s^{-1}). The photons from the source are attenuated by a 6 mm thick lead sheet. A cavity (4 cm diameter x 10 cm depth) along the cylindrical axis of the assembly allows exposing the detector to the thermalized neutron field. The neutron field in the point of test at the centre of the cavity was simulated with MCNPX 2.6. Table 1 resumes the results of the simulation. The neutron spectrum is reported in Fig. 9. It should be noted that the epithermal and fast components of the spectrum represent approximately half of the neutron fluence, but their contribution to the TNRD reading is only 1.6%. The Cadmium-ratio for the TNRD is in fact in the order of 60.

Figure 8. The moderating cylinder used to test and calibrate the TNRDs. The Am-Be source is located on top of the cylinder and is shielded with a 6 mm lead sheet.

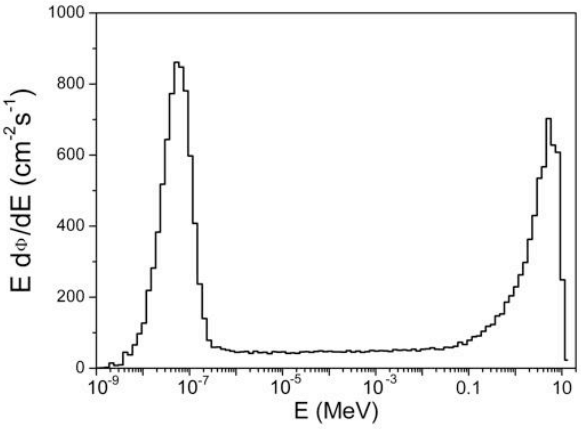

Figure 9. The neutron spectrum at the point of test located at the centre of the moderating cylinder shown in Fig. 7.

The direction distribution of the thermal fluence in the calibration cavity of the moderating cylinder was determined through MCNPX simulations and represented in Figure 10. Here the quantity $\Delta\Phi_{th}$, defined as the conventional thermal fluence from μ and $\mu+\Delta\mu$, is reported as a function of $\mu = \cos(\theta)$. θ is the angle formed by particle direction and the axis joining the point of test with the neutron source. It can be seen that the field is not isotropic, with a factor of approx. two from m = -1 to m = 0.

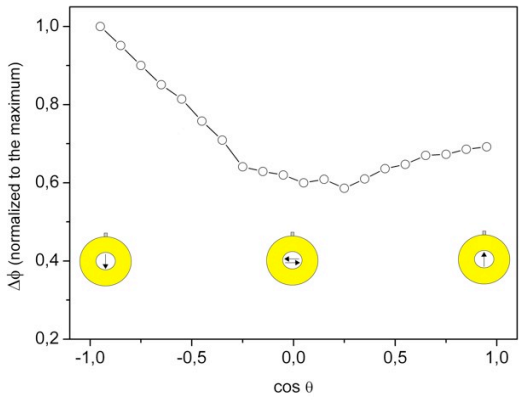

Figure 10. Direction distribution of the thermal fluence in the calibration cavity of the moderating cylinder determined through MCNPX. Values are normalized to the maximum, corresponding to the top-down direction. Arrows in the sketch indicate particle trajectories at the point of test.

After manufacturing, every TNRD is exposed at the point of test of the moderating cylinder to measure its response to thermal neutrons. Typical response is (96±3) $cm^{-2}s^{-1}$ mV^{-1} in terms of conventional thermal flux. To estimate the reproducibility of the manufacturing process, the response of ten TNRDs with nominally identical fabrication characteristics was compared, and its variability is 5% (one s.d.).

The response to photon radiation, measured in a reference ^{137}Cs field, is (0.51±0.02) mGy h^{-1} mV^{-1}.

An experimental campaign at the ENEA Casaccia TRIGA reactor allowed evaluating the response linearity of the TNRD in the range from 7E+2 to 3E+5 $cm^{-2}s^{-1}$ (corresponding to reactor power from 500 W to 200 kW). The results are shown in Fig. 12. The stability of the neutron yield from the reactor, evaluated on the basis of the fixed monitor instruments (the so called "linear amplifiers") ranged from ±1% to ±3%.
Uncertainties on the conventional thermal flux measured with the TNRD are the quadratic combination of two contributions, coming from the TNRD calibration in the moderating cylinder (±3%) and from the reading statistics in the reactor field. The latter obviously decreases as the reactor power increases. Its value is ±6% at 500 W and lowers to less than ±1% at 5 kW. This can be understood by comparing Figure 7 (obtained at 46 kW) with Figure 11 (0.5 kW).

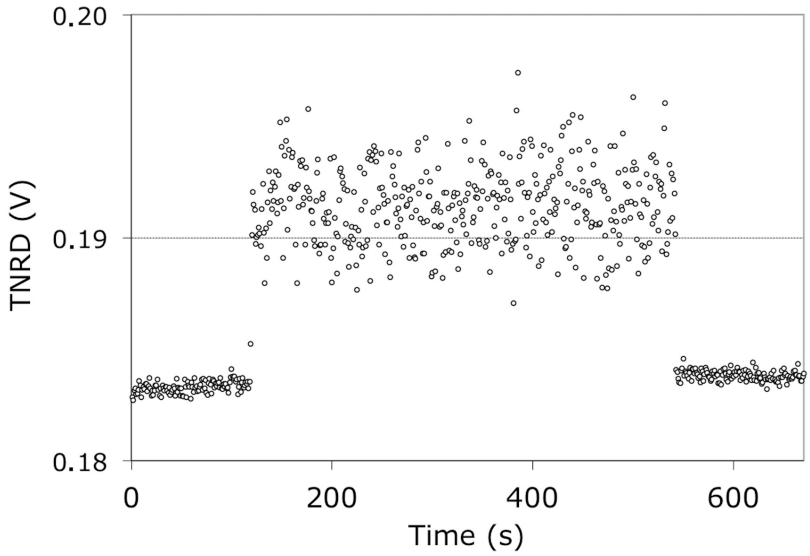

Figure 11. Time-dependent output of the TNRD when exposed in an ex-core thermal neutron beam from the ENEA Casaccia TRIGA reactor at power 0.5 kW. The step is produced when opening and closing the neutron shutter.

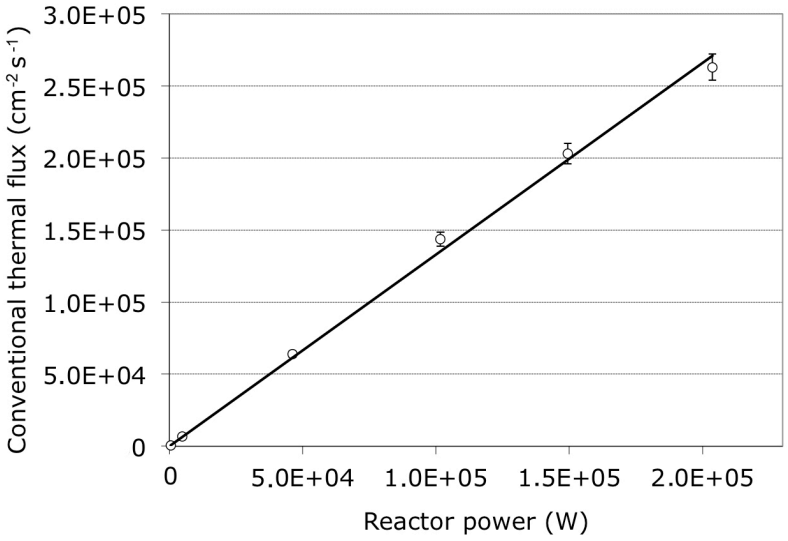

Figure 12. Linearity curve of the TNRD acquired at the TRIGA reactor (ENEA Casaccia).

The isotropy of the TNRD response was tested by rotating the detector in the calibration cylinder. The measured values are constant within ±3%, thus indicating a good level of isotropy. Further experiments in a mono-directional thermal field are planned to complete this study.

3.5 *CYlindrical SPectrometer (CYSP)*

3.5.1 Built prototype and in-lab testing

The CYSP spectrometer has been designed according to the conclusions of a detailed simulation study made with MCNPX 2.6 [5], using the ENDF/B-VII cross-section library [6] for neutrons with energies below 20 MeV and the room temperature cross-section tables in polyethylene, S(α,β). Neutron transport above 20 MeV has been modelled using Bertini intra-nuclear cascade model and Dresner evaporation model [7]. The CYSP spectrometer mainly consists of a series of TNDs (thermal neutron detectors) located along the axis of a polyethylene cylinder that provides spectral information when it is irradiated with a directional neutron beam.

The dimensions of the cylinder as well as the location of detectors have been optimized to achieve spectral resolution and practically eliminate the eventual contribution from epithermal neutrons coming from lateral directions. The collimator and the additional shielding made in borated plastic are included to eliminate such lateral contributions over the whole energy range.

As it is shown in Figure 13, the first part of the CYSP is a collimator 50 in diameter 30 cm in length made of polyethylene. The hole diameter is 16 cm and it is covered by 5 mm thick borated plastic SWX-238. The central capsule of the spectrometer (on the right in figure) is a 35 cm diameter polyethylene cylinder with seven detectors located along the axis. Detector-to-detector distance along the cylindrical axis is 2 cm approximately. A lead disk has been inserted between 6th and 7th positions to increase the response to high-energy neutrons. Air holes are needed to favour streaming of neutrons towards deep measurement positions. The response matrix is given in Fig. 14. The signal of every detector is reported, per unit incident fluence, as a function of the monochromatic neutron energy. Detector 1 is the shallowest and detector 7 is "behind lead", thus its response increases above approx. 1 MeV. The detectors located near the lead filter (above and below) respond to high-E neutrons because secondary neutrons from n,xn reactions are also emitted at large angles.

A prototype of the CYSP was fabricated, equipped with active detectors and tested in the neutron field from an Am-Be source (emission 2.09×106 s-1) at the INFN-LNF. See Fig. 15 for the irradiation set-up.

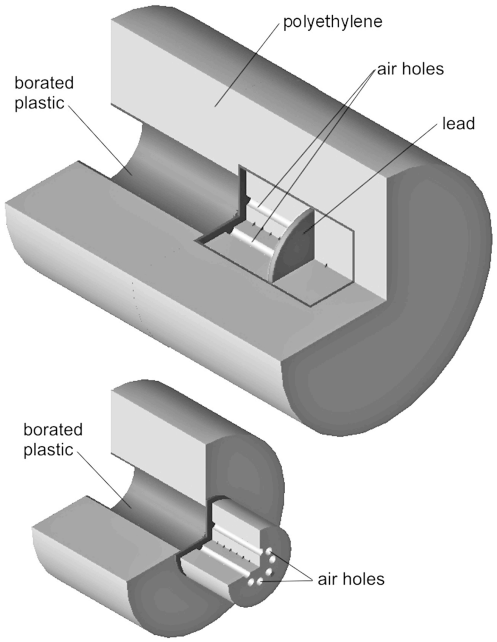

Fig. 13. Scheme of the CYSP.

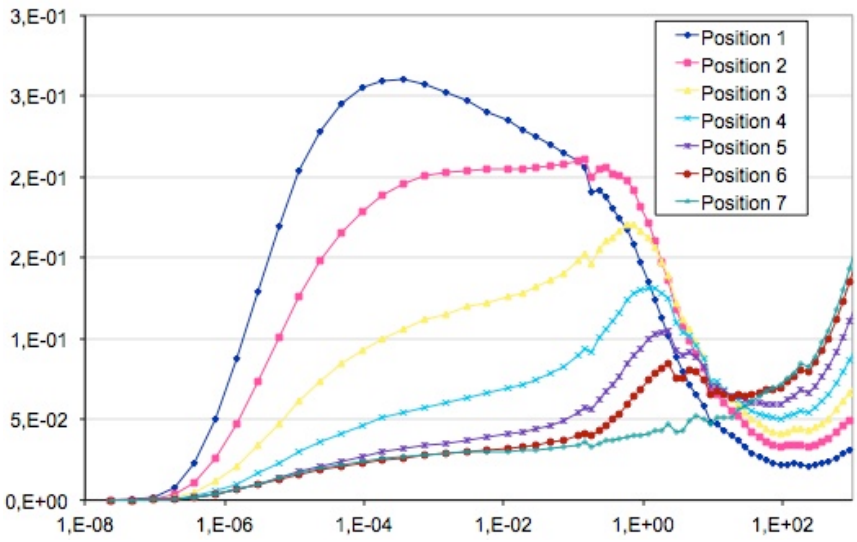

Figure 14. Typical response matrix of the CYSP.

Fig. 15. Irradiation set-up of the CSYP at the INFN-LNF. The source is on top.

A high-scatter scenario, shown in Fig. 15, was intentionally chosen with the aim of verifying the directionality of the CYSP response. This test included both simulations and experiments:

(1) The readings of the detectors placed at seven different depths along the CYSP axis were simulated in absence and presence of the walls, ceiling and floor of the irradiation room. The difference is lower than 1% for positions 1 to 5, and 1%-2% for the deeper positions 6 and 7.

(2) The CYSP was irradiated for about one week and the detector readings were compared with those expected from the simulation. The experimental count rates varied from 0.09 s^{-1} (position 7) to 0.29 s^{-1} (position 2). The coherence between measured and simulated response is shown in Fig. 16. The error bars combine the counting statistics and the response matrix overall uncertainty. The latter contribution provisionally was set to ±3% on the basis of previous experience with the Bonner spheres (to be confirmed with the data of the NPL experiment with mono-chromatic beams). The standard deviation of the ratio between measured and expected reading over the seven measuring positions is 2%, thus demonstrating the accuracy of the simulation model.

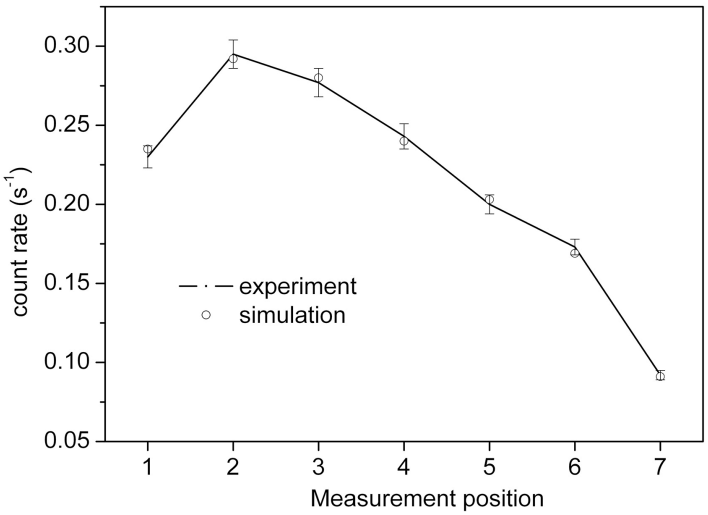

Figure 16. Profile of the count rate along the seven measurement positions of the CYSP. Uncertainty bars are ~3%.

3.5.2 NPL experiment with mono-chromatic beams

Irradiations took place from 28 Oct, 2013 to 1st Nov, 2013 at NPL (Teddington, UK). The mon-chromatic energies were 0.144 MeV, 0,565, 2.0, 3.5, 5.0, 16.5 MeV in addition to a reference ^{252}Cf source. To eliminate the response due to air- and room-scattered neutrons, the device was calibrated using the shadow-cone technique, implying the difference of two measurement: one taken in total field minus another taken in presence of a shadowing shield, called shadow-cone (20 cm of iron followed by 30 cm polyethylene, arranged in a cone-shaped device covering the source-to-detector solid angle).

As an example, see in Fig. 17 the pulse-height-spectra obtained in the seven detectors when exposing the CYSP to 2 MeV neutrons.

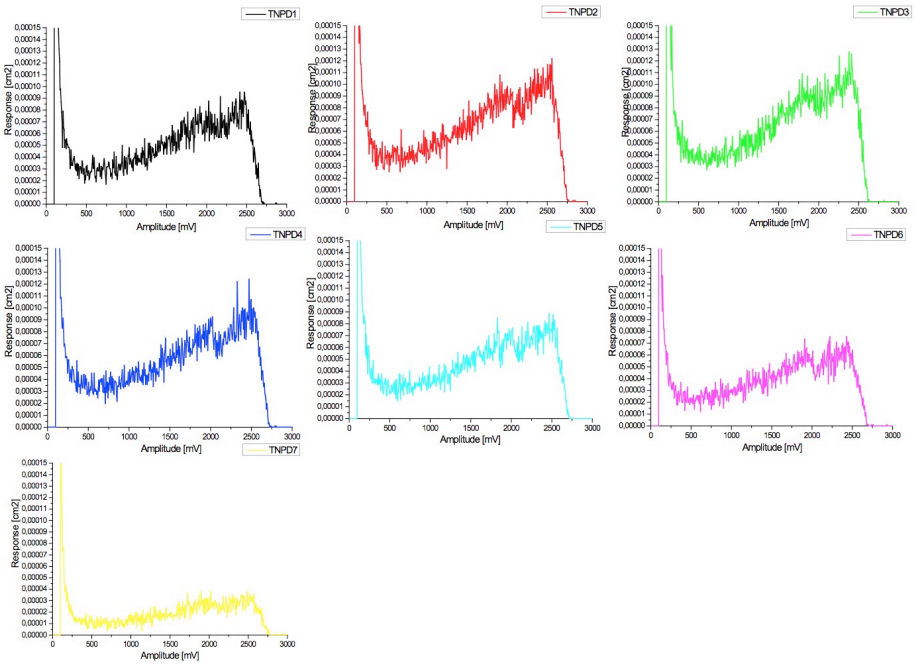

Fig. 17. The pulse-height-spectra obtained in the seven internal detectors when exposing the CYSP to 2 MeV neutrons. TNPD1 indicates thermal neutron pulse detector n. 1, located in the shallowest position. TNPD7 is the deepest position, behind the lead filter.

All spectra from Fig. 17 were acquired using the board of Fig. 3, especially developed within NESCOFI for multi-detector instruments.

The thermal neutron-induced events are included in the double-peaked structure located around 2 V in the pulse height spectra of Fig. 17. These are separated from the photon background through a simple threshold placed at about 0.6 V. The net thermal neutron signal for each detector, i.e. the number of counts per second above the threshold, was calculated for every detector and for every mono-chromatic energy. This response matrix was compared with the theoretical response matrix derived with MCNPX.

The profiles of Fig. 18 prove the strict correspondence between simulated and experimental response matrix.

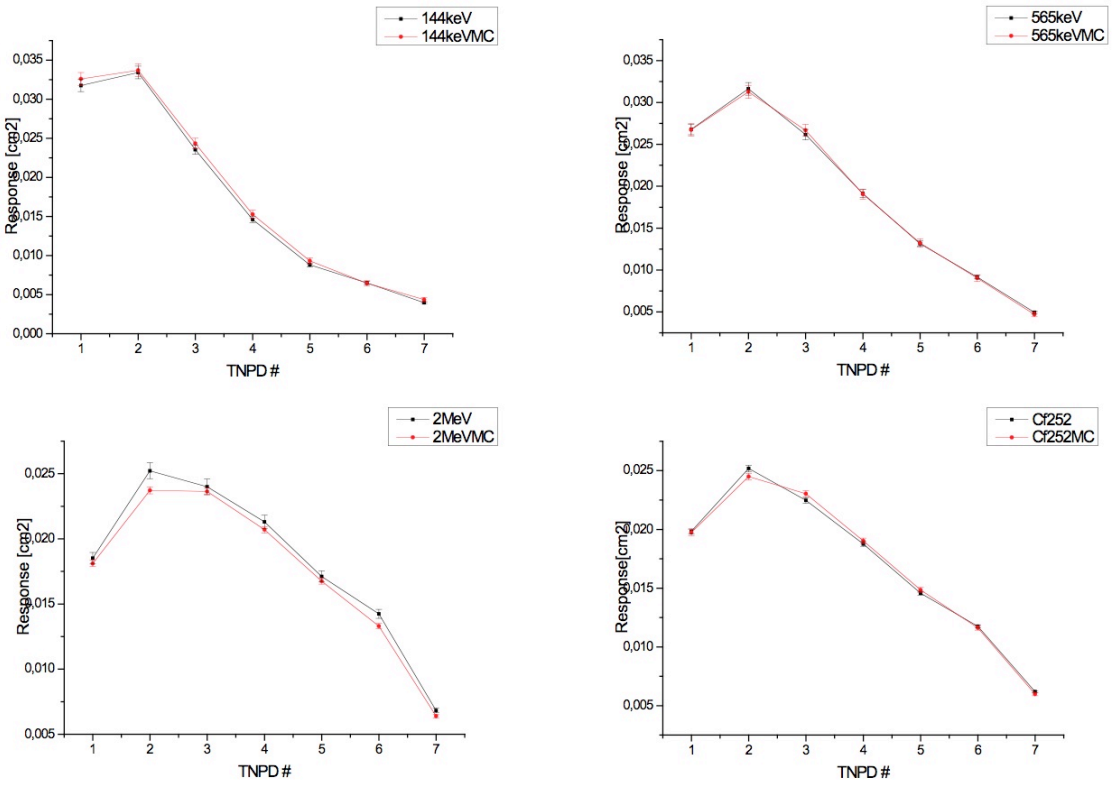

Figure. 18. Comparison bewtween simulated and experimental response of the CYSP, as a function of detector position (TNPD #) and irradiation energy (only 144 keV, 565 keV, 2 MeV and ^{252}Cf profiles are shown).

The ratio between experimental and calculated response represents the instrument calibration factor. If the response matrix is well simulated, this number should not vary as the detector position and irradiation energy vary. This was checked on the basis of the results shown in Table 2. The calibration factor was separately derived, for each energy, by averaging the ratios obtained from all detectors (columns of the Table). The result does not vary with energy (within 2-3% uncertainty). A best estimation of the calibration factor was obtained as weighted average (inverse variance taken as weight) of all values and its uncertainty is lower than 2%.

The CYSP testing and calibration task can be now regarded as concluded with a really good level of confidence and very low uncertainties.

	144 KeV	565 keV	2 MeV	3,5 MeV	5 MeV	16,5 MeV	Cf-252
1	0,195	0,200	0,204	0,196	0,202	0,214	0,201
2	0,198	0,202	0,213	0,201	0,206	0,205	0,206
3	0,194	0,196	0,203	0,193	0,193	0,194	0,195
4	0,191	0,201	0,206	0,188	0,199	0,193	0,197
5	0,189	0,199	0,204	0,184	0,194	0,190	0,196
6	0,201	0,203	0,214	0,190	0,199	0,203	0,202
7	0,182	0,210	0,214	0,199	0,199	0,204	0,207
Average	0,193	0,202	0,208	0,193	0,199	0,200	0,201
Uncertainty	3,2%	2,2%	2,4%	3,2%	2,3%	4,2%	2,3%

Weighted average	0,200
Weighted unc.	1,35%

Table 2. CYSP calibration Table.

3.6 *The SPherical Spectrometer (SP^2)*

3.6.1 Response matrix and passive prototype

The SP^2 spectrometer consists of thirty-one thermal neutron detectors arranged along three perpendicular axes at 5 radial distances (5.5, 7.5, 9.5, 11 and 12.5 cm) and at the centre of a polyethylene sphere of diameter 25 cm. An internal 1 cm thick lead shell between 3.5 and 4.5 works as an energy converter via (n,xn) reactions thus enhancing the response above 20 MeV, either for the central detector and for those located at 5.5 and 9.5 cm.

Although the response of a single TND in a given location is clearly not isotropic, a nearly isotropic response is obtained by averaging the readout of detectors located at the same radial response, as it has been discussed in previously published papers [8,9]. The same works also demonstrate the spectrometric capabilities of the device from thermal energies up to hundreds MeV neutrons.

The SP^2 response matrix, intended as the response of each thermal neutron detector per unit incident fluence as a function of the detector position and the irradiation energy, was modelled on the basis of extensive simulations performed with MCNPX 2.6 Monte Carlo code. To validate these calculations, a passive prototype, operating with Dysprosium activation foils, with was built in 2011 and tested in reference monochromatic fields available at PTB. The energies were 0.147, 0.565, 1.2, 5.0 and 14.8 MeV The details of the experimental campaign are reported in [10].

As a main result, the activation profile along the X-axis of the SP^2 (coinciding with the irradiation direction, see Fig. 19) was studied and compared with the "expected" one, i.e. the activation profile obtained by folding the SP^2 simulated response matrix with the reference neutron spectra. According to the results, shown in Figure 20, it can be concluded that the simulated response matrix satisfactorily predicts the experimental spectrometer response for all investigated neutron energies. It should be noticed that the position corresponding to the maximum of the profile shifts toward deeper positions as the energy

increases. This effect constitutes the basis for using SP^2 as a neutron spectrometer.

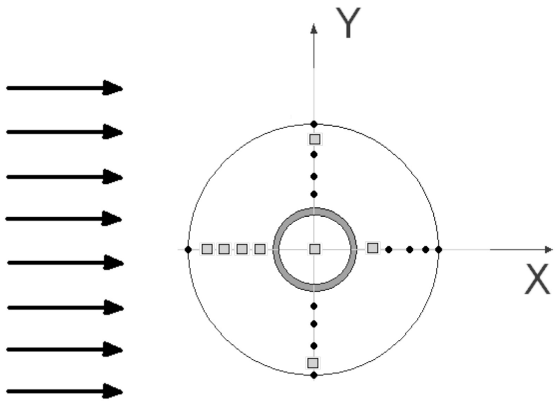

Figure 19. Irradiation geometry for testing the passive prototype with monochromatic reference neutron fields.

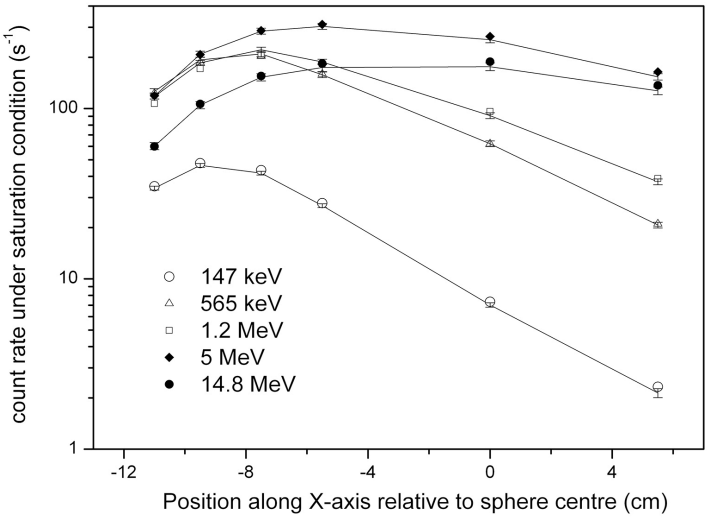

Figure 20. Saturation count rate measured in the Dysprosium activation foils exposed in the selected positions of SP2 for the 0.147, 0.565, 1.2, 5.0 and 14.8 MeV (continuous lines). The expected count rates, obtained from the simulated response matrix, are also reported (symbols). Only the measurement positions along the X-axis of SP2 were considered.

3.6.2 Active prototype calibration

The active prototype was achieved in May 2013. Active thermal neutron detectors of type TNPD have been embedded in the 25 cm diameter polyethylene + lead sphere, and arranged as sketched in Fig. 21. Detectors occupy positions at radius = 0 (centre), 5.5 cm, 7.5 cm, 9.5 cm, 11 cm, 12.5 cm (on surface). As in the case of the CYSP spectrometer, signals from detectors were acquired through NESCOFI multi-detector board (see Fig 3) and digitized with NI USB 6366 digitizer.

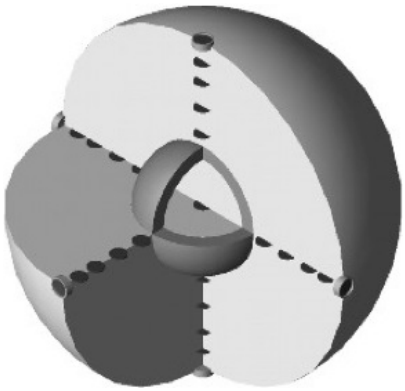

Figure 21. Geoemtry of the SP2 with detector positions. Only one detector is located behind the lead insert. Detectors on surface are back-shielded with 1 mm of Cd with the aim of preventing a possible signal due to neutrons backscattered from the sphere.

Taking advantage of the reference ^{241}Am-Be source available at FISMEL laboratories of INFN-LNF, a partial calibration of the SP2 was achieved using the shadow-cone technique. See Fig. 22 for the irradiation geometry using the shadow cone (source to cone distance 3 cm; source to sphere-centre distance 100 cm).

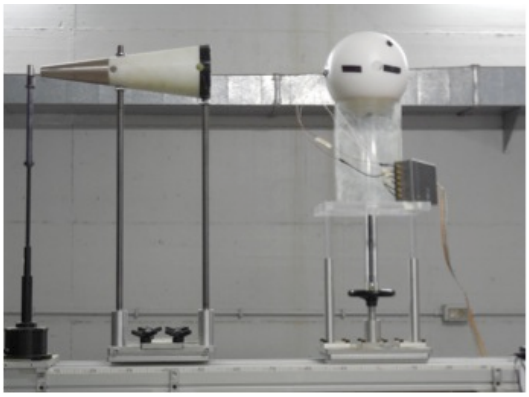

Fig.2. Irradiation geometry with the shadow cone.

Differently than CYSP, the Spherical Spectrometer responds to neutrons coming from all directions, thus well defined irradiation geometries were fixed for calibration purposes. These irradiation geometries are

reported in Fig. 23 and are only referred to the six detectors located along a specified radius of the sphere (evidenced in figure).

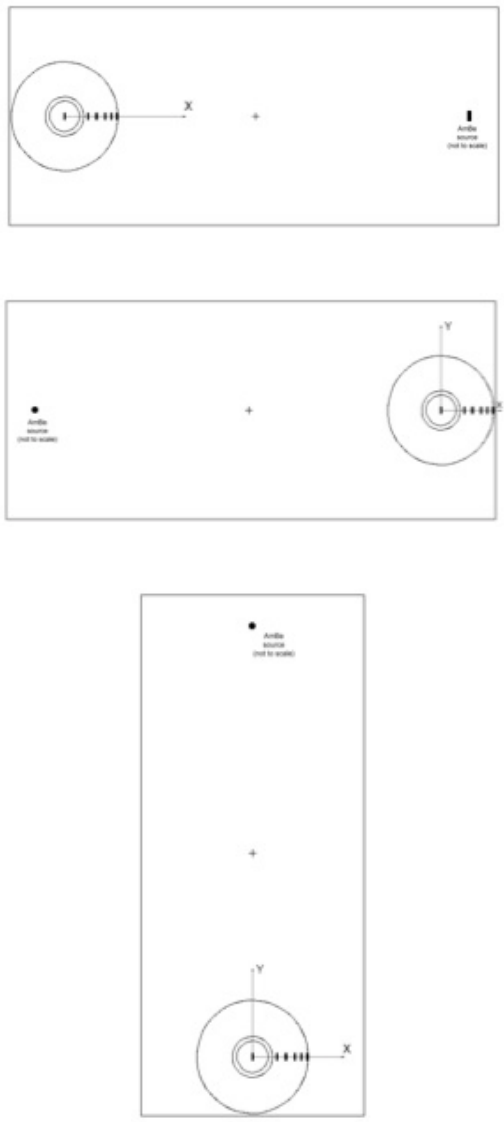

Fig. 23. Irradiation geometries chosen for calibrating the active version of the SP^2. From top to down: (1 0 0), (-1 0 0), lateral.

For every irradiation geometry two exposures, with and without shadow-cone, were performed. The net count rates (total measurement – cone measurement) in the six selected detectors were then compared with those obtained from the MCNP simulation, obtaining the profiles of Figure 24 Uncertainties on individual are in the order of 5%. The experimental profiles satisfactorily agree with the simulated ones. The SP^2 calibration factor, defined as the weighted average of all experimental/simulated count ratios, is 0.185 ± 2%.

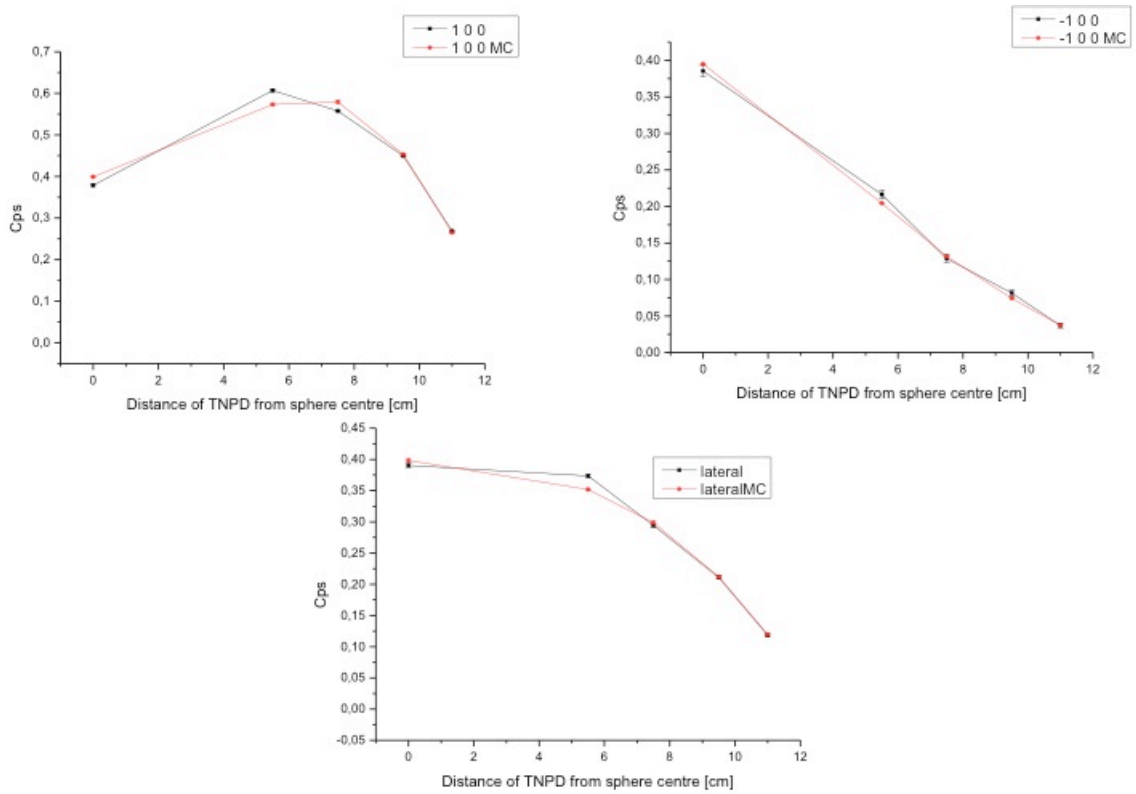

Figure 24. Exposure to Am-Be reference field. Count rate in the SP^2 as a function of the detector position and of the irradiation geometry. Only the six detectors located along the sphere radius forming the indicate geometry are considered.

3.6.3 Field test of the SP^2

A field test was organized at the 14.6 MeV quasi monochromatic beam of the ENEA fast neutron generator, obtained at 45° from a T(d,n) target (deuterium energy 260 keV). The irradiation set-up is shown in Figure 25. According to the formalism described in Para. 3.6.2, the (1 0 0) geometry was tested. The experimental and expected profiles are compared in Figure 26. Within the uncertainties (in the order of 10% for the neutron emission, 2% for the response matrix, 3 to 5% for the experimental count rate), the experimental readings are well predicted by the simulation. The difference from the nominal neutron fluence and that derived from the experimental profile was 3%.

Figure 25. The irradiation set-up at ENEA Fast neutron Generator.

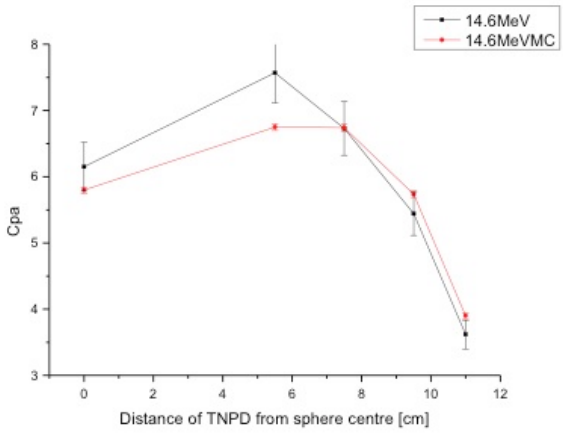

Figure 26. Experimental and expected profiles for SP2 irradiation at ENEA Fast neutron Generator.

3.7 *Applying the TNRD in the medical sector*

A collaboration with Sevilla University, Azienda Ospedaliera San Camillo-Forianini (Roma) and Ospedale Santa Maria delle Croci (Ravenna) consolidated the use of TNRD in the in-phantom neutron dose measurements during photon radiotherapy sessions. This allowed validating a recently developed risk model for the neutron-induced second cancer in patients [11]. Figure 27 shows the NORMA anthropomorphic phantom used for the validation experiment. This phantom was submitted to two standard 15 MV treatments, in abdomen and head (See Fig. 28 for the different gantry positions, corresponding to fractions with equal dose to the isocentre). The TNRD was exposed in four selected point of interest (center of head, lung, abdomen and skin) obtaining the results of Table 3.

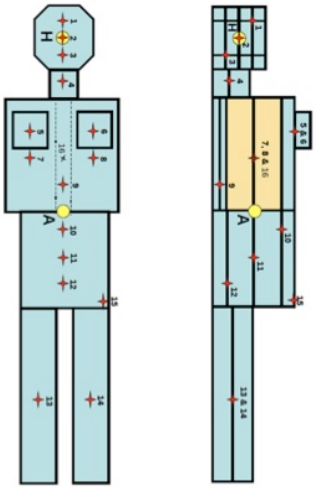

Figure 27. The NORMA anthropomorphic phantom used for the validation experiment.

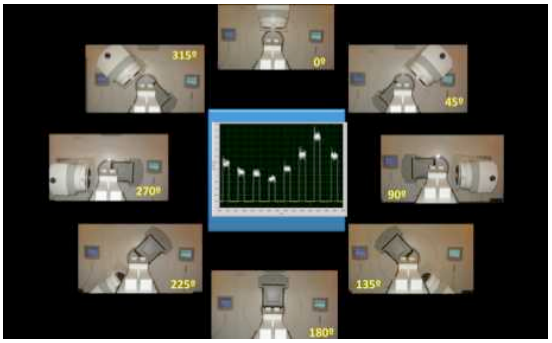

Figure 28. Gantry positions for a typical treatment and corresponding DC signal from the TNRD.

Table 1. Intercomparison of termal fluence for Head & Neck treatment (10^7 cm^{-2}/MU)

Point/organ	TLD	TNRD	Monte Carlo	SRAM
Lung (#8)	3.6±0.2	3.41±0.17	2.71	4.75
Abdomen (#11)	0.38±0.02	0.39±0.02	0.39	0.25
Skin (#15)	2.1±0.1	2.1±0.1	0.71	0.87

Table 2. Intercomparison of termal fluence for Abdomen treatment (10^7 cm^{-2}/MU)

Point/organ	TLD	TNRD	Monte Carlo	SRAM
Head	2.63±0.13	2.90±0.14	2.29	2.8
Lung (*)	4.1±0.6	4.2±0.2	3.33	7.7
Abdomen (*)	1.10±0.16	0.92±0.05	1.05	1.5
skin	3.5±0.2	3.1±0.2	1.05	2.2

Table 3. Thermal neutron fluence measrurements in the four selected organs for head and neck or abdomen treatments. The TNRD response is here compared with passive systems (TLDs), simulations or calculations based on a the reading of an "ambient" detector (SRAM).

Following the satisfactorily results from this test, the system formed by a single TNRD and its DAQ electronics was extended to five parallel detectors working in parallel to simultaneously measure neutron doses in multiple organs (Co-funded by Sevilla University).

3.8. *Collaboration and external funds*

CIEMAT Madrid: 35,000 equiv-hours CPU time on EULER cluster. A contract for building a dedicated SP2 for CIEMAT is under elaboration.

CRISP (INFN-LNF): 6 k€ (detectors, trips exp. campaigns)

Politecnico di Milano 3 k€ (trips at experimental campaigns) + support for electronics design and testing

Sevilla Universiy: 3 k€ co-funding for parallelization of the TNRD fro medical sector.

Azienda Ospedaliera San Camillo-Forianini (Roma) and Ospedale Santa Maria delle Croci (Ravenna): usage of 15 MV electron LINACs

LNF support:
- 2 man*month at mechanical workshop
- Guest-house: 30 man*night
- Experiments for detector fabrication and characterization performed at FISMEL laboratories.

3.9. *Project meetings*

29 Jan 201, LNF, 2013 NESCOFI launch meeting
15 April 2013, Milan, Mid-year NESCOFI meeting.

3.10 *International Review Panel*

Text of the 2013 reviewer reports

"*It is my pleasure for me to write this letter to truly recommend this project for medical benefits. NESCOFI achieved the stated targets on time and on budget. Looking from thepoint of view of the medical sector, where we are involved, we see important applications for the developed instruments. This is especially true for the present and coming years, due to the increasing interest of the medical community for the second*

cancers induced by neutrons in radiotherapy patients. The availability of real-time spectrometers, like those developed in the project, would allow to extensively map the oncology accelerator facilities, thus leading routine patient-risk assessment practices which will benefit a significant fraction of population. We recommend to specialize (maybe simplify, considering the reduced energy range of medical linacs) a version of SP^2 for the medical sector only). Concerning in-phantom neutron evaluations, we tested the miniaturized thermal neutron detectors of type TNRD in our phantom NORMA, with promising results in terms of rapidity, accuracy and possibility to multiply the number of simultaneous measurement points. I hope my letter will help you to take a decision. Please do not hesitate to contact me if you have further questions. Yours Sincerely"

Prof. Francisco Sanchez Doblado, Profesor Catedratico Universidad de Sevilla, paco@us.es

"Dear Dr. Bedogni,

It is a pleasure for me to confirm that the project was able to reach a satisfactory level of testing and calibration for both spectrometers in spite of the economical restrictions. The impressive results obtained with CYSP, especially the high degree of accuracy and the significant response differentiation as a function of the energy, suggest that its use in neutron beam-lines or for cosmic rays would produce important and new results. The SP2 has the potentiality for opening the way to a new philosophy of neutron area monitoring for radiation protection, and for this reason I recommend to further develop it, possibly in conjunction with an industry. Results are clear, complete, and produced on time".

Prof. Carles Domingo, Profesor Titular Universitat Autonoma de Barcelona, carles.domingo@uab.cat

3.11 *Web-site*

http://www.lnf.infn.it/acceleratori/public/nescofi/

3.12 *2013 Publications*

Main publications for 2013 are:
NIM A 714 (2013) 110-114.
Radiat. Meas. 50 (2013) 67-70
Radiat. Meas. 50 (2013) 78-81
IEEE Trans. Nucl. Sci. 60 (6) (2013) 4692-4696.

Most of the activity done in 2013 was presented at the 12th Neutron and Ion Dosimetry Symposium (NEUDOS-12), Aix en Provence, 3-7 June 2013. The project obtained one session chair, four orals and three posters. Paper published in 2014.

The applications to medical sector were presented to the SEFM 19 - SEPR 14 (18-21 June 2013, Caceres, Spain) with an invited talk and a poster.
NESCOFI activity was also presented to the Giornata di studio su IRIDE (10-11 June 2013, LNF) and at the Workshop HeRe in Italy, 2-3 Dec. 2013 (ENEA Frascati).

4. Bibliography

[1] Bedogni, R., Domingo, C., Esposito, A., Fernandez, F., 2007. FRUIT: an operational tool for multisphere neutron spectrometry in workplaces. Nucl. Instr. Meth. A 580, 1301 1309.

[2] Bedogni, R., Pelliccioni, M., Esposito, A., 2010. A parametric model to describe neutron spectra around high-energy electron accelerators and its application in neutron spectrometry with Bonner Spheres. Nucl. Instr. Meth. A 615, 78-82.

[3] A. Pola, D. Bortot, M.V. Introini, R. Bedogni, A. Gentile, A. Esposito, J. M. Gomez-Ros, E. Passoth, A. Prokofiev. Compact thermal neutron sensors for moderator-based neutron spectrometers. Radiation Protection Dosimetry (2014). doi:10.1093/rpd/nct298.

[4] R. Bedogni, D. Bortot, A. Pola, M. V. Introini, A. Gentile, A. Esposito, J. M. Gomez-Ros, M. Palomba, A. Grossi. A new active thermal neutron detector. Radiation Protection Dosimetry (2014). doi:10.1093/rpd/nct319.

[5] Pelowitz, D.B. (ed.). MCNPX User's Manual Version 2.6. Report LA-CP-07-1473 (2008).

[6] Chadwick, M.B., Oblozinsky, P., Herman, M. et al. Evaluated Nuclear Data File ENDF/B-VII.0. Nuclear Data Sheets 107, 2931-3118 (2006).

[7] Pioch, C., Mares, V., Rühm, W. Influence of Bonner sphere response functions above 20 MeV on unfolded neutron spectra. Radiat. Meas. 45, 1263-1267 (2010).

[8] Gómez-Ros, J.M., Bedogni, R., Moraleda, M., Delgado, A., Romero, A., Esposito, A. A multi-detector neutron spectrometer with nearly isotropic response for environmental and workplace monitoring. Nucl. Instrum. Meth. A 613, 127-133 (2010)

[9] Gómez-Ros, J.M., Bedogni, R., Moraleda, M., Esposito, A., Pola, A., Introini, M.V., Mazzitelli, G., Quintieri, L., Buonomo, B. Designing an extended range single-sphere multi-detector neutron spectrometer. Nucl. Instrum. Meth. A 677, 4-9 (2012)

[10] Bedogni, R., Gómez-Ros, J.M., Pola, A., Introini, M.V., Bortot, D., Gentile, A., Esposito, A., Mazzitelli, G., Quintieri, L. , Buonomo, B. Testing a newly developed single-sphere neutron spectrometer in reference monochromatic fields from 147 keV to 14.8 MeV. Nucl. Instrum. Meth. A 714, 110-114 (2013).

[11] F. Sánchez-Doblado; C. Domingo; F. Gómez; B. Sánchez-Nieto; J.L. Muñiz; M.J. García-Fusté; M.R. Expósito, R. Barquero; G. Hartmann; J.A. Terrón; J. Pena; R. Méndez; F. Gutiérrez; F.X. Guerre; J. Roselló; L. Núñez; L.Brualla-González; F. Manchado; A. Lorente; E. Gallego; R. Capote; D. Planes; J.I. Lagares; X. González-Soto; F. Sansaloni; R. Colmenares; K. Amgarou; E.

Morales; R. Bedogni; J.P. Cano; F. Fernández.Estimation of neutron-equivalent dose in organs of patients undergoing radiotherapy by the use of a novel online digital detector. Phys. Med. Biol.57,pp. 6167 – 6191 (2012).